Vision Research 207 (2023) 108209

Contents lists available at ScienceDirect

Vision Research

journal homepage: www.elsevier.com/locate/visres

Increasing spatial frequency of S-cone defined gratings reduces their visibility and brain response more than for gratings defined by L-M cone contrast

Rebecca Lowndes [a,b,*], Lauren Welbourne [a,b], Molly Williams [a], Andre Gouws [a,b], Alex Wade [a,b,c], Antony Morland [a,b,c]

[a] Department of Psychology, University of York, United Kingdom
[b] York Neuroimaging Centre, University of York, United Kingdom
[c] York Biomedical Research Institute, University of York, United Kingdom

A B S T R A C T

Chromatic sensitivity reduces as spatial frequency increases. Here, we explore the behavioural and neuronal responses to chromatic stimuli at two spatial frequencies for which the difference in sensitivity will be greater for S-cone than L-M stimuli. Luminance artefacts were removed using the Random Luminance Modulation (RLM) technique. As expected, doubling the spatial frequency increased the detection threshold more for S-cone than for isoluminant L-M gratings. We then used fMRI to measure the cortical BOLD responses to the same two chromatic stimuli (S and L-M) at the same two spatial frequencies. Responses were measured in six visual areas (V1, V2, V3, V3a, hV4, TO1/2). We found a significant interaction between spatial frequency in V1, V2 and V4 suggesting that the behaviourally observed increase in contrast threshold for high spatial frequency S-cone stimuli is reflected in these retinotopic areas. Our measurements show that neural responses consistent with psychophysical behaviour in a colour detection task can be observed as early as primary visual cortex.

1. Introduction

It has been long established that human colour vision is trichromatic (Young, 1802, Von Helmholtz, 1867). Long after those historical works, it was found that cone photoreceptors in the human eye had different spectral absorptions (Brown and Wald, 1964; Bowmaker and Dartnall, 1980), having three cone classes tuned to long (L) medium (M) and short (S) wavelengths. These three cones form three visual pathways; L+M (achromatic luminance channel), L-M (red-green) and S-(L+M) (blue-yellow) (MacLeod and Boynton, 1979) demonstrated in the Lateral Geniculate Nucleus (LGN) of primates (Wiesel & Hubel, 1966; Derrington, Krauskopf, & Lennie, 1984). Early psychophysical work investigated contrast sensitivity as a function of spatial frequency along red-green and blue-yellow colour directions and found that sensitivity is reduced as spatial frequency increases (Mullen, 1985). The chromatic pathways in the LGN have since been more accurately described as red-cyan (L-M) and lavender-lime (S-(L+M)) (Conway, 2009). The reduction in sensitivity for high spatial frequency chromatic gratings has been replicated more recently for both L-M and S colour directions (Mullen & Kingdom, 2002, Welbourne, Morland & Wade, 2018, Neitz et al., 2020, Wuerger et al., 2020). Work above threshold in colour matching tasks has shown that pattern sensitivity is lower in S-cone than L-M conditions (Poirson and Wandell, 1993). Other work has confirmed that the difference in threshold between high and low spatial frequencies is more pronounced for gratings defined along the S than the L-M cardinal colour directions (Poirson and Wandell, 1996, Mullen and Kingdom, 2002).

Work by Williams and colleagues (1993) investigated whether these differences were due to optical factors or neural sampling effects. Optical factors are any factors relating to the eye such as chromatic aberration, which causes colour distortion, and differences in quantum catch, which is the effect of the reduced number of S-cones in the human retina when compared to L and M cones. They showed that the reduction in sensitivity caused by optical factors to S-cone and L-M stimuli was largely the same across spatial frequencies, particularly those below 4 cpd. They found that neural factors affected L-M and S-cone sensitivity at similar rates at 4 cpd and above. Between 2 (the lowest spatial frequency tested) and 4 cpd, there is a hint that there is a greater reduction in sensitivity for S-cone compared to L-M stimuli. Other work (Swanson, 1996) has shown that S-cone contrast sensitivity can be relatively independent of non-neural factors when measured between 1 and 5 cpd using an extension of two-colour increment threshold techniques developed by Stiles (1946). Later work has shown using quick contrast

* Corresponding author.
E-mail address: rebecca.lowndes@york.ac.uk (R. Lowndes).

https://doi.org/10.1016/j.visres.2023.108209
Received 19 May 2022; Received in revised form 30 January 2023; Accepted 31 January 2023
Available online 4 March 2023

sensitivity functions that binocular summation of chromatic stimuli depends on neural processing and not optical factors up to 2.5 cpd (Kim et al., 2017). The current study aims to investigate neural factors and has adopted a method inspired by the work of Stiles using backgrounds to ensure targets are detected by single chromatic neural mechanisms.

The human occipital lobe has multiple retinotopic representations, which can be identified with fMRI (DeYoe et al., 1994; Sereno et al., 1995; Engel, Glover & Wandell, 1997). The largest representation is striate cortex (V1) (Dougherty et al., 2003), which receives input from the LGN. Beyond V1, lie V2, V3, V3a and hV4, which have been shown to exhibit preferential responses to different stimuli. Colour appears to drive responses in ventral occipital area hV4, first identified in humans by Zeki and colleagues (1991). Area V3a lies on the dorsal surface and has a similar topography and the same hierarchical position as hV4 in the visual cortex. V3a, is more commonly associated with motion selectivity (Tootell et al., 1997; Klaver et al., 2008; Mikellidou et al., 2018) and has shown a significant preference for achromatic stimuli (Mullen et al., 2007) as well as high temporal frequency flicker (Liu and Wandell, 2005). However, other work has shown dorsal involvement in colour processing, including V3a (Liu & Wandell, 2005; Mullen, Thompson and Hess, 2010; D'Souza et al., 2011, Castaldi et al., 2013). Further along the dorsal stream lie TO1 and TO2, the retinotopic analogue of MT+ (Amano, Wandell, & Dumoulin, 2009), the human motion area. These visual field maps are considered to be motion selective and show lower responses to chromatic stimuli than achromatic stimuli (Mullen et al., 2007; Wandell et al., 1999).

While many studies have shown that ventral visual areas, including hV4, are very sensitive to colour stimuli (Zeki et al., 1991; McKeefry & Zeki, 1997; Wade, Brewer, Rieger & Wandell, 2002; Goddard et al., 2011; Mullen, Chang and Hess, 2015; Mullen, 2019), the findings do not mean that substantive chromatic processing is not undertaken in earlier visual areas such as V1 (Mullen et al., 2007). In fact, studies have shown chromatic processing is a common feature in early visual areas (Railo et al., 2012; Mullen et al., 2015; Mullen, 2019); an fMRI adaptation study showed all early visual areas showed responses to both coloured and achromatic stimuli (Mullen, Chang and Hess, 2015; Mullen, 2019). Careful examination of responses to colour modulations in V1 and V2 (Engel, Zhang and Wandell, 1997) showed a coupling between fMRI BOLD responses to coloured gratings and psychophysical detection thresholds, for some, but not all stimulus conditions.

Using fMRI to link neuronal responses and perception is challenging. To optimise signal quality in fMRI, stimuli are normally presented above threshold and over a relatively large spatial area. The former means that inaccurate specification of cone stimulation values can result in small but significant luminance artefacts. The latter means that accurate specification of cone stimulation is challenging because of the spatial variations of spectrally selective absorption in the macular pigments (Ruddock, 1963; Snodderly, Auran & Delori, 1984; Hammond, Wooten, & Snodderly, 1997; Chen, Chang and Wu, 2001; Davies and Morland, 2004) and morphology of cone outer segments (Goodchild, Ghosh and Martin, 1996; Srinivasan et al., 2008) across eccentricities of the retina. Chromatic aberration can also induce luminance artefacts, particularly at high spatial frequencies (Murasugi and Cavanagh, 1988; Bradley, Zhang and Thibos, 1992). To overcome these challenges, we adopted the approach taken by Birch, Barbur and Harlow (1992), who presented colour stimuli superimposed on a rapidly updating grid of checks with random luminance values. This Random Luminance Modulation (RLM) reduces the sensitivity of the achromatic pathways. This renders luminance artefacts undetectable and therefore allows responses to chromatic content of stimuli to be isolated. This specific technique has not yet been used fMRI experiments, though Wade and colleagues (2008) used a similar technique to demonstrate robust responses to colour stimuli in human ventral cortex.

In this study we first aimed to determine whether the lower sensitivity to high spatial frequency S-cone grating stimuli compared to their L-M counterparts could be established psychophysically in the presence of an RLM background. We measured sensitivity to square wave gratings on an RLM background at two spatial frequencies (1.25 and 2.5 cycles per degree (cpd)) for two colour directions (S-cone and L-M). Relatively low spatial frequencies were chosen to reduce the effects of longitudinal chromatic aberration, which are more pronounced as spatial frequency increases (Murasugi and Cavanagh, 1988; Bradley, Zhang and Thibos, 1992). We found grating contrast sensitivity at 2.5 cpd was reduced compared to 1.25 cpd grating and that this reduction in sensitivity was greater for S-cone than L-M gratings. Suprathreshold versions of the four grating stimuli were presented to participants during acquisition of fMRI data. We assessed responses from six retinotopic representations (V1, V2, V3, V3a, hV4 and TO1/2) to determine at what levels of the cortical hierarchy we might observe processing consistent with the contrast sensitivities we measured. We found an interaction between spatial frequency and colour direction - that followed our contrast sensitivity measures - in V1, V2 and, in one experiment V4, which was driven by the greater difference between responses to high and low spatial frequency stimuli defined along the S-cone compared to L-M colour directions. The responses we measured in these areas were therefore consistent with the behavioural data and likely indicate that the mechanism limiting detection of coloured gratings is set at or before primary visual cortex.

2. Methods

2.1. Participants

2.1.1. Behavioural experiment

Six (four female) colour-normal trichromats (confirmed with a Rayleigh match) with a mean age of 33.5 years (+- 11.00 years) were recruited for a single 40-minute psychophysics session in the scanner. The ethics committee at York Neuroimaging centre at the University of York approved this experiment.

2.1.2. FMRI experiments

Six (four female) colour-normal trichromats (confirmed with a Rayleigh match) with a mean age of 25.7 years (+- 5.47 years) were recruited. All participants took part in five hour-long fMRI sessions. The ethics committee at York Neuroimaging centre at the University of York approved these experiments.

2.2. Experiment and stimulus design

2.2.1. Target stimuli

Target stimuli (Fig. 1) were square wave gratings in the central 10x10 degrees squared of either low spatial frequency (1.25 cpd) or high spatial frequency (2.5 cpd). The spatial frequencies tested in this experiment were carefully chosen to ensure that any results found could not be explained exclusively by the effects of longitudinal chromatic aberration, which has a strong influence at high spatial frequencies (Murasugi and Cavanagh, 1988; Bradley, Zhang and Thibos, 1992). Some evidence suggests that the effects of longitudinal chromatic aberration are negligible below 4 cpd (Pefferkorn, Chiron & Vienot., 1997) which is beyond the highest spatial frequency of the current study at 2.5 cpd. To examine this more thoroughly, we used the equation detailed by Strasburger et al (2018) to calculate the diameter of blur given as:

$$b^{\circ} = 0.057PD$$

where P is the pupil diameter in millimetres and D is the defocus in diopters. A different project in our lab used the same contrast RLM background as the current project, but recorded videos of the eyes of participants. We found in 6 participants that pupil diameter was 3.19 mm on average. Rynders, Navarro, and Losada (1998) calculated D over similar wavelengths (458–632 nm) to the limits of the projector used in the current study (455–625 nm) and found D to be equal to ±0.5 over the eccentricities used in our stimuli. Therefore, the diameter of blur is

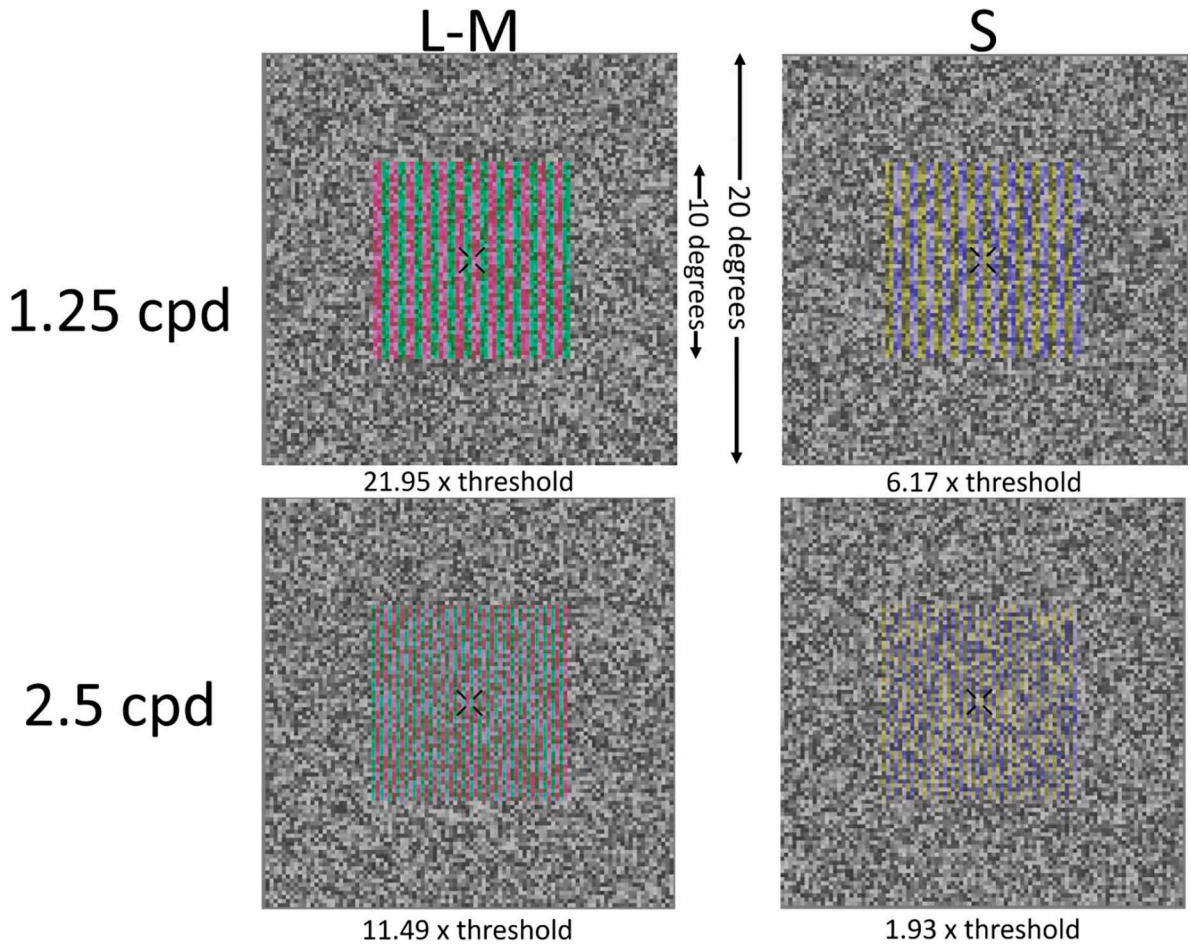

Fig. 1. Images of the stimuli that were presented during experiments. Note that target gratings are shown at a higher contrast for demonstration purposes. The multiples of threshold shown below are based on the mean threshold found for each condition from the behavioural experiment described in 2.2.4 and 3.1, with a contrast of 2.7% in the L-M condition and 10.5% in the S-cone condition. Fixation is shown here as was present during the fMRI experiments.

equal to 0.091. The blur would therefore extend 0.045 degrees on either side of the grating boundary. Given that the grating bar width has a minimum of 0.2 degrees, blur extending from each boundary (2 × 0.045 degrees) leaves the majority of the bar, 0.109 degrees, unaffected by blurr and therefore at the specified contrast.

Chromatic contrasts of the targets (2.7% L-M and 10.5% S-cone) were chosen for the fMRI experiments based on multiples of the behavioural thresholds found in the behavioural experiment outlined in 2.2.4 and 3.1. An fMRI study by Mullen et al (2007) found surprisingly high responses to S-cone stimuli at lower (5x) multiples of threshold in comparison with similarly high responses to L-M stimuli at much higher (31x) multiples of threshold. We reasoned therefore that selecting stimulus contrasts that should elicit similar fMRI responses for L-M and S-cone stimuli at 1.25 cycles per degree would offer the best way to examine effects associated with doubling spatial frequency. We therefore chose values of ~ 22x (21.95) multiples of threshold for L-M (equating to 2.7%) and ~ 6x (6.17) multiples of threshold for S-cone (equating to 10.5%). We erred on the side of caution insofar as relative to Mullen et al (2007) our S-cone stimuli may be anticipated to yield greater response than those to L-M stimuli. Moreover, these values were also high enough that our high spatial frequency targets (2.5 cpd) in both chromatic conditions were still visible (11.49 multiples of threshold for L-M and 1.93 multiples of threshold for S-cone).

2.2.2. Random luminance modulation (RLM) stimuli

The stimuli used for the RLM background were adapted from Birch and colleagues (1992). The background stimulus consisted of an array of squares, in which each check was assigned a greyscale value between ±50% L+M contrast from the uniform grey field at random every 0.05 s (20 Hz). This background subtended 20x20 degrees square of visual angle and remained on for the duration of each scan. The rationale for the design is to have a rapidly updating, relatively high luminance (mean luminance 177 cd/m^2) contrast component to the stimulus, to which luminance sensitive mechanisms will respond robustly. Any small luminance artefacts resulting from colour modulations superimposed on the background should therefore be undetected by luminance sensitive mechanisms.

2.2.3. Stimulus presentation

The visual stimuli were designed and presented using PsychoPy and PsychToolBox in MATLAB. The delivery system used for the visual stimulus in the scanner was a ViewPixx projector, which projected the stimulus onto a custom-made acrylic screen. The participant viewed the screen with a mirror fixed to the head coil in the scanner. Spectral measurements of the RGB channels of the scanner screen were made using a 'Jaz' (Ocean Optics, FL) spectrometer. Chromatic stimuli were defined using the 10-deg cone fundamentals based on the Stiles and Burch 10-deg colour matching functions described in Stockman and Sharpe (2000). These values allowed us to specify isoluminant S and L-M cone stimuli for the average observer using silent substitution. No further accounting for luminance for the individual participants in this study was conducted, so if presented on a uniform background the gratings we generated could contain luminance artefacts. However, the random luminance modulation described in 2.2.2 is an effective way of

rendering many of these artefacts invisible.

2.2.4. Behavioural experiment

Behavioural experiments were performed inside the scanner bore using a two-interval forced choice paradigm. The RLM background comprised an array of 100x100 squares (0.2x0.2 degrees squared) (Fig. 1) which remained on throughout the duration of the experiment. Target stimuli were chromatic gratings in the central 10x10 degrees squared of either low spatial frequency (1.25 cpd, comprising bars of width equal to two background checks) or high spatial frequency (2.5 cpd, comprising bars of width equal to one background check). Fixation changed from standard (+) to cross (x) for 0.5 s when the target stimulus could be present. Targets were separated by a 2 s interval, with one target containing a chromatic grating, and one without but still showing the RLM background. Participants were asked to press '1′ if the target was in the first presentation of 'x' and '2′ if it was in the second presentation. A standard three-up one-down staircase was used to adjust the target contrast. The task finished after 16 reversals or 100 trials. The ~ 80% threshold was calculated as the mean of the contrast during the last 7 reversals.

2.2.5. fMRI experiment 1: RLM background (0.2x0.2 squared degree checks)

In the first fMRI experiment, the background comprised an array of squares (100x100) covering an area of 20x20 degrees squared (Fig. 1) - identical to that used in the behavioural experiments. Each element of the array subtended 0.2 × 0.2 degrees of visual angle. Target gratings were superimposed over the RLM background which added either chromatic contrast (L-M contrast at 2.7%, S-cone contrast at 10.5%) or, in a control experiment, achromatic contrast (L+M contrast at 15%), in a square wave pattern. As before, stimuli at two spatial frequencies were presented; 1.25 cpd and 2.5 cpd. The orientation of the target grating was vertical and contrast polarity was reversed at 1 Hz. The choice of reversal rate of the target stimulus increases the likelihood that colour specific mechanisms dominate the response to the colour modulations, as they have sluggish temporal response properties (Regan and He, 1996, Wade et al., 2008), particularly for S-cone stimuli (Liu & Wandell, 2005). Each block-design fMRI run consisted of a single combination of three potential chromatic conditions and two potential spatial frequency conditions presented eight times with a cycle time of 30 s. Each cycle contained a 15 s grating presentation with RLM background and fixation marker and 15 s of RLM only with a fixation marker. In each session, lasting approximately one hour, all six combinations of stimulus spatial frequency and colour direction were presented. Each participant completed three sessions resulting in 18 h of scan data.

To help participants maintain fixation during the fMRI experiments, they performed a demanding attentional task (button press when the fixation cross changed width) which was not locked to the timing of the stimuli.

2.2.6. fMRI experiment 2: RLM background (0.4x0.4 squared degree checks)

In order to establish whether any effects were due to the change in spatial frequency, or the change in spatial concordance with the RLM background, all participants also completed a further one-hour scan session with the background checks set to 0.4 deg rather than the original 0.2 deg. This meant that the 1.25 cpd grating matched the RLM background spatially. The target gratings followed the same colour directions (L-M, S-cone and L+M) at one spatial frequency of 1.25 cycles per degree. Participants completed the same fixation task as described in 2.2.5. Each chromatic condition was presented in two runs in one scanning session leading to six scans in a session. Each run followed the block design described above.

2.2.7. Retinotopy stimuli

The retinotopy scans used a sweeping bar stimulus, which were similar to those described in other experiments (Dumoulin and Wandell 2008; Binda, Thomas, Boynton, & Fine, 2013; Alvarez et al., 2015; Welbourne, Morland & Wade, 2018). Specifically, our bars were 1.25 degrees of visual angle wide, and moved in 16 steps across a 20 degrees diameter circular aperture, for 8 bar directions (with four blank periods); the order of the bar directions and positions of the blank periods was as described in Welbourne, Morland and Wade (2018). Each bar step lasted for the length of one TR (2500 ms), and contained a 100% contrast white noise stimulus, which had been scaled by a factor of 8 to reduce the average spatial frequency in the texture. The texture updated at 2 Hz. Participants carried out four repeats of these scans in one scan session. To aid participants in maintaining central fixation, participants performed an attentional task (button press when the fixation point changed colour) that was not locked to the timing of the stimuli. The scan session for the retinotopy lasted for approximately 40 min and comprised four runs.

2.3. MRI protocol

All scans were carried out using a Siemens 3 T MRI scanner, with a 64-channel head coil. The participant's head was positioned in the coil with foam padding to ensure the head was stable. For the functional scans, 76 EPI slices were taken within an FOV of 192x192mm with 1.5 mm isotropic voxels (TR = 2500 ms, TE = 40.8 ms, flip angle = 75 degrees, voxel matrix = 128x128). Scan slices were aligned axially and always covered occipital and temporal lobes.

In addition to the functional scans, three T1-weighted and two T2-weighted structural scans were taken for each participant, at a 0.8x0.8x0.8 mm resolution. The protocol for these scans was taken from the Human Connectome Project (Glasser et al., 2013).

2.4. Data processing

2.4.1. Structural - data processing

All structural scans were analysed using the HCP minimal processing pipeline (version 5.0, (Glasser et al., 2013) using a combination of FSL (http://fsl.fmrib.ox.ac.uk/fsl/fslwiki/ (Smith et al., 2004) and Freesurfer (http://surfer.nmr.mgh.harvard.edu/ (Dale, Fischl & Sereno, 1999; Reuter, Schmansky, Rosas, & Fischl, 2012)).

TO1 and TO2 were derived using the anatomically defined retinotopy atlas (Benson et al., 2014) implemented in the python analysis toolbox 'neuropythy' (Benson and Winawer, 2018). The atlas then predicted several Freesurfer-based maps (visual area, eccentricity, polar angle, and pRF size), which were used to delineate the central 5 degrees of TO1 and TO2 which were then combined into a single ROI referred to as TO1/2 for further analysis.

2.4.2. Retinotopy - data processing

Population receptive field (pRF) mapping was performed using the 2015 version of the VISTA software (https://web.stanford.edu/group/vista/cgi-bin/wiki/index.php/Software) (Vista Lab, Stanford University), running under MATLAB 2015 (The MathWorks Inc., Natick, MA, USA). We applied pRF modelling to an average of all retinotopy scans which had been motion corrected between and within scans using a maximum likelihood alignment routine (Nestares and Heeger, 2000). Functional scans were aligned to individual anatomy scans using FLIRT linear registration (Jenkinson and Smith 2001; Jenkinson, Bannister, Brady, & Smith, 2002). The retinotopic eccentricities and polar angles extracted by the pRF model were then used to draw boundaries of visual areas V1, V2, V3, V3a and hV4 on a flattened representation of visual cortex (see Fig. 2); for details of the pRF model used see Welbourne et al (2018). These regions of interest (ROIs) were then restricted to the central 5 degrees of eccentricity to best fit the stimuli (10 deg diameter) and transformed into NIFTI files using the VISTA function roiSaveAsNifti for use in the rest of the analysis, which was performed in FSL (see below).

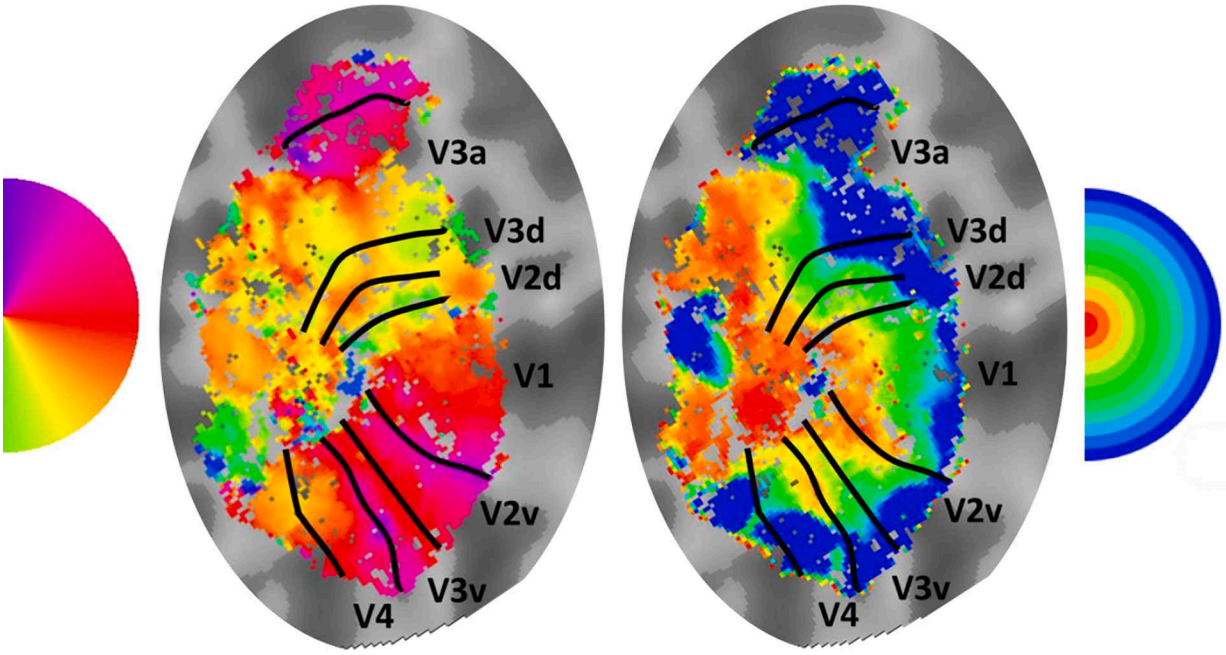

Fig. 2. The retinotopic maps used to delineate ROIs for one participant with phase map (left) and eccentricity map (right) for the left hemisphere. Visual area boundaries are overlaid on the maps.

2.4.3. fMRI experiments - data processing

The data for all fMRI experiments other than retinotopy detailed in 2.4.2 were pre-processed using FEAT (FMRI Expert Analysis Tool) version 6.00, part of FSL (FMRIB's Software Library) version 5.0. Images were skull-stripped using a brain extraction tool (BET (Smith, 2002)). Motion correction (MCFLIRT; (Jenkinson, Bannister, Brady, & Smith, 2002)) was followed by spatial smoothing (Gaussian full width half maximum 2 mm). Data were high pass temporal filtered (Gaussian-weighted least-squares straight line fitting with sigma = 15.0 s). Individual participant data was registered to their own high resolution structural (generated from T1 and T2 structural images using the HCP processing pipeline) using FLIRT (12 DOF, Jenkinson and Smith, 2001; Jenkinson, Bannister, Brady, & Smith, 2002). Time-series statistical analysis was carried out using FILM with autocorrelation correction (Woolrich, Ripley, Brady, & Smith, 2001).

For each run for each participant, two explanatory variables were defined. The first modelled our target as 15 s on and 15 s of blank. The second modelled each time the task appeared on screen. The target model was our main effect and the task was modelled as a variable of no interest. Percentage signal change was then computed for each run, each visual area and in each participant individually using FeatQuery. Signal change values for runs of the identical conditions were then averaged for each participant.

3. Results

3.1. Behavioural results

We first assessed whether a doubling of the spatial frequency of the chromatic gratings from 1.25 to 2.5 cpd reduced the sensitivity more to S compared to L-M contrast. The sensitivity (1/cone contrast threshold) for detecting chromatic gratings superimposed on the luminance-modulated background are shown in Fig. 3. Doubling the spatial frequency decreased sensitivity to gratings modulated along both cardinal colour directions (Fig. 3 left panel). Every participant tested demonstrated greater difference between S-cone than L-M contrast sensitivity (Fig. 3 right panel). A 2x2 ANOVA revealed a significant interaction between colour condition and contrast threshold ($F(1, 5) = 7.83$, $p = .038$, $\eta^2 = 0.61$) which is driven by the greater loss of sensitivity to high spatial frequency S-cone stimuli consistent with the literature (Mullen, 1985; Mullen and Kingdom, 2002; Poirson and Wandell, 1993; 1996; Welbourne, Morland and Wade, 2018). Brain regions that perform chromatic processing that underpin the behavioural measures should therefore show an interaction in the BOLD response between the spatial frequency and colour axis of the gratings.

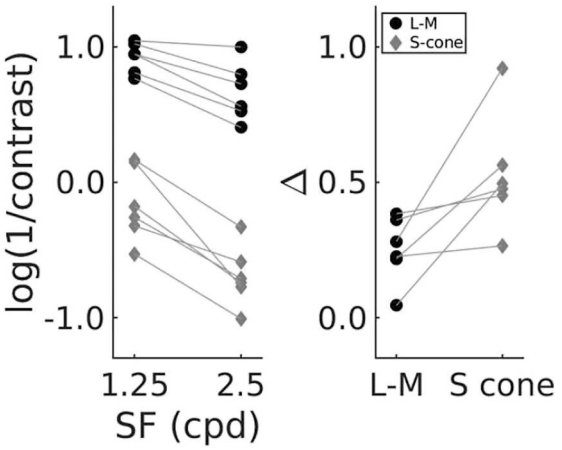

Fig. 3. Left panel: A graph to show the inverse log of the cone contrast thresholds (~80% correct) for L-M and S-cone conditions at the test spatial frequencies of 1.25 and 2.5 cpd. The dots and diamonds represent each participant's individual threshold and lines are drawn between each participant's threshold at each spatial frequency. Right panel: A graph showing the difference (Δ) between sensitivities shown in the left panel at 1.25 cpd and 2.5 cpd for L-M and S-cone conditions. Dots represent the difference for each participant and lines are drawn between their L-M and S-cone Δ values.

3.2. fMRI results

Based on the behavioural data, we hypothesised that the effect of doubling spatial frequency would be more pronounced for BOLD

responses to S-cone targets compared to L-M targets. Given that different visual areas have different sensitivities to both colour and spatial frequencies, we also asked whether this interaction might also depend on the cortical location from which we record responses. Such an effect would be indicated by a three-way interaction between visual field map, chromaticity and spatial frequency.

Responses to the four chromatic stimulus conditions acquired for each visual field map are shown in Fig. 4. It appears that the reduction in response resulting from a doubling of spatial frequency is greater for S than L-M stimuli in all regions of interest apart from TO1/2. To assess whether effects varied by visual field map, we ran a three-way repeated measures ANOVA (see table 1) which revealed a significant three way interaction between visual area, colour direction and spatial frequency. There was a significant two-way interaction between colour direction and spatial frequency, likely driven by the fact that all but one (TO1/2) visual area showed the same pattern of response. Also noted is the interaction between visual area and spatial frequency, again likely caused by the responses in TO1/2.

To follow-up on the three-way interaction we performed two-way ANOVAs on the responses from each visual field map. Significant interactions between colour axis and spatial frequency were found in V1 ($F(1, 5) = 11.26$, $p = .020$, $\eta^2 = 0.69$;) and V2 ($F(1, 5) = 9.75$, $p = .026$, $\eta^2 = 0.66$) but not in V3 ($F(1, 5) = 3.30$, $p = .129$, $\eta^2 = 0.40$), V3a ($F(1, 5) = 1.50$, $p = .275$, $\eta^2 = 0.23$) or TO1/2 ($F(1, 5) = 0.76$, $p = .422$, $\eta^2 = 0.13$) with V4 ($F(1, 5) = 6.34$, $p = .053$, $\eta^2 = 0.56$) approaching significance.

Given the markedly small responses from TO1/2 we checked to see whether they differed from zero with single sample t-tests. The TO1/2 response only differed from zero for the high spatial frequency L-M condition ($T(5) = 3.14$, $p = .026$).

While the responses we recorded to gratings defined along cardinal colour axes fitted with our predictions in some visual field maps we still wanted to check that the modulation of the background minimised the chance of detecting responses to luminance artefacts in our stimuli. To do this, we presented gratings defined by L+M contrast superimposed on the modulating background. The gratings were at a contrast that was high (15%) relative to any expected luminance artefact. The responses to target gratings at 1.25 and 2.5 cpd are shown for each visual field map in Fig. 5. The responses at 2.5 cpd were not significantly different from zero, but responses to the low spatial frequency grating appear larger, although notably smaller than responses we recorded to coloured gratings of the same spatial frequency. The results indicate that small luminance artefacts are unlikely to register responses that would unduly affect the responses we attribute to chromatic modulations of our targets. To investigate potential effects we applied a two-way repeated measures ANOVA, which showed a significant interaction between the effect of spatial frequency and visual field map ($F(5,25) = 6.31$, $p = .020$, $\eta^2 = 0.56$). There could be an issue therefore in terms of how the difference between the spatial frequency of the target and background reduces the masking of the background. Pairwise comparisons reveal that this effect appears to be driven by V1 ($F(1, 5) = 9.73$, $p = .026$, $\eta^2 = 0.66$) and V2 ($F(1, 5) = 7.08$, $p = .045$, $\eta^2 = 0.59$) as all other areas showed a non-significant effect of the spatial frequency of achromatic stimuli (V3: $F(1, 5) = 2.04$, $p = .212$, $\eta^2 = 0.29$; V3a: $F(1, 5) = 0.50$, $p = .512$, $\eta^2 = 0.09$; hV4: $F(1, 5) = 1.01$, $p = .360$, $\eta^2 = 0.17$; TO1/2: $F(1, 5) = 2.10$, $p = .207$, $\eta^2 = 0.30$). It is reassuring that in the high spatial frequency condition there is no significant response to 15% contrast L+M gratings as a source of a luminance artefact in chromatic conditions is chromatic aberration, which is increasingly problematic as spatial frequency increases (Murasugi and Cavanagh, 1988; Bradley, Zhang and Thibos, 1992).

To check whether the partial release from the masking of the background (when target and background are not matched) could have caused the interaction between chromatic condition and spatial frequency we performed an experiment in which we increased the size of the background checks to 0.4 squared degrees, which matched the width of the coarser (1.25 cpd) target grating's bars. We compared the target related responses to this stimulus configuration with those originally obtained with the background check size of 0.2 squared degrees as shown in Fig. 6. In all visual field maps the responses obtained with the smaller background checks were greater than those obtained with background checks that matched the width of the target gratings irrespective of the colour of those gratings. However, if the change in response to the target resulting from the change in the background varied by colour direction, this could contribute to the interaction between spatial frequency and colour direction we detected earlier. We therefore ran a three-way repeated measures ANOVA (Table 2), which showed no significant interaction between colour direction and spatial frequency of the background and no significant three-way interaction between colour direction, spatial frequency and visual area which shows that the different target and background spatial properties that we originally used are unlikely to be the cause of the interaction between colour direction and spatial frequency that we observed earlier (Table 1).

In the knowledge that increasing the background check size reduced the response to the low spatial frequency target grating, notwithstanding the absence of an interaction between background check size and colour direction, we chose to be cautious and compare responses to target grating of different spatial frequencies and colour directions under conditions where the background checks matched the bar widths of the target gratings. The spatial frequency of the target gratings are therefore identical to those shown in Fig. 4. The responses obtained under these matched conditions are shown in Fig. 7. The reduction in response caused by the doubling of spatial frequencies is still clearly evident for S-cone stimuli, but is now less clear for L-M stimuli. It appears therefore, that the larger cost of increasing spatial frequency for S-cone than L-M cone defined grating persists. To check this we ran a three-way ANOVA as we did before (Table 3). There was a significant three-way interaction between visual field map, spatial frequency and colour axis and the same two-way interaction between spatial frequency and colour axis as found for the main experiment. Follow-up two-way ANOVAs applied for each visual field map - to investigate the source of the three-way interaction - showed significant interactions between colour axis and spatial frequency in all visual field maps apart from V3a

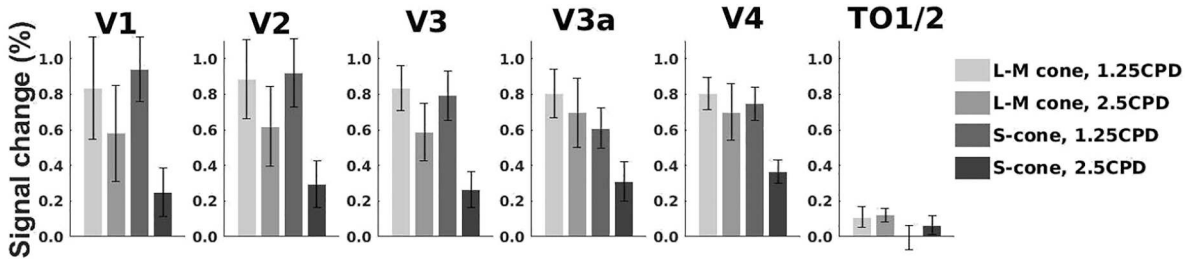

Fig. 4. A bar graph to show the mean percent signal change to each spatial frequency (1.25 and 2.5 cpd) for each colour direction (L-M and S-cone) for each visual area. Error bars are one standard error of the mean (SEM).

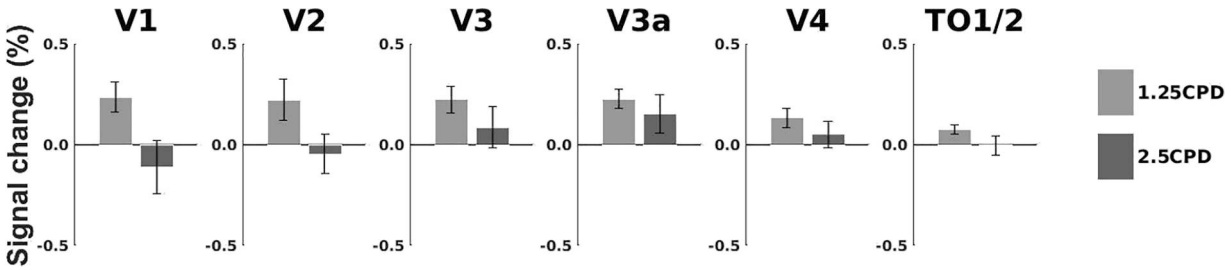

Fig. 5. Bar graphs to show the percentage signal change to achromatic stimuli at both spatial frequencies (1.25 and 2.5 cpd). Error bars are one SEM.

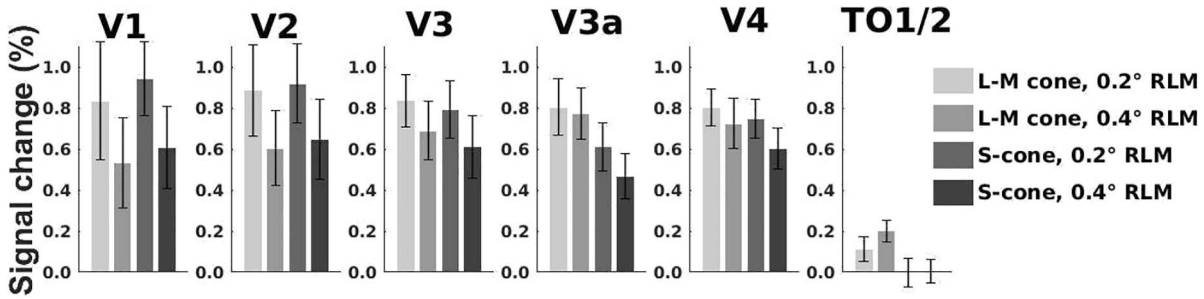

Fig. 6. A bar graph to show the mean percent signal change to the lower spatial frequency target (1.25 cpd) on the high spatial frequency and low spatial frequency background (0.2 and 0.4 degrees squared checks) for each colour direction (L-M and S-cone) for each visual area. Error bars are one SEM.

Table 1
Results of the ANOVA to investigate effects of visual areas (V1, V2, V3, V3a, hV4 and TO1/2), chromatic condition (L-M and S-cone) and spatial frequency (1.25 and 2.5 cpd) on the BOLD response. Greenhouse-Geisser correction is applied when sphericity is violated.

Source	Mauchly's *p*	df1, df2	F	*p*	Effect Size
Area (A)	0.099	5, 25	7.57	**<0.001**	0.60
Chromatic Condition (B)	.	1, 5	8.05	**0.036**	0.62
Spatial Frequency (C)	.	1, 5	41.71	**0.001**	0.89
A × B	**0.012**	1.52, 7.60	1.37	0.299	0.22
A × C	0.073	5, 25	10.88	**<0.001**	0.69
B × C	.	1, 5	6.67	**0.049**	0.57
A × B × C	0.203	5, 25	3.92	**0.009**	0.44

Table 2
Results of the ANOVA to investigate effects of visual areas (V1, V2, V3, V3a, hV4 and TO1/2), chromatic condition (L-M and S-cone) and spatial frequency of the RLM background (0.2 and 0.4 degrees squared checks, 1.25 cpd target grating) on the BOLD response. Greenhouse-Geisser correction is applied when sphericity is violated.

Source	Mauchly's *p*	df1, df2	F	*p*	Effect Size
Area (A)	**0.009**	1.37, 6.86	8.59	**<0.001**	0.63
Chromatic Condition (B)	.	1, 5	2.17	0.201	0.30
Background Spatial Frequency (C)	.	1, 5	8.85	**0.031**	0.64
A × B	0.169	5, 25	7.44	**<0.001**	0.60
A × C	**<0.001**	1.51, 7.56	6.93	**0.024**	0.58
B × C	.	1, 5	0.26	0.631	0.05
A × B × C	0.053	5, 25	0.38	0.920	0.05

and TO1/2 (V1: $F(1, 5) = 6.82$, $p = .048$, $\eta^2 = 0.58$; V2: $F(1, 5) = 7.90$, $p = .038$, $\eta^2 = 0.61$; V3: $F(1, 5) = 7.13$, $p = .044$, $\eta^2 = 0.59$; V3a: $F(1, 5) = 2.10$, $p = .207$, $\eta^2 = 0.30$; hV4: $F(1, 5) = 19.24$, $p = .007$, $\eta^2 = 0.79$; TO1/2: $F(1, 5) = 5.81$, $p = .061$, $\eta^2 = 0.54$). The significant interactions are driven by the lower responses elicited by the high spatial frequency S gratings compared to their lower spatial frequency counterparts and gratings defined by modulation along the L-M colour axis. The results indicate again that the doubling of the target grating's spatial frequency reduces responses to stimuli defined by modulations along the S more than those defined by modulations along the L-M axis.

4. Discussion

The aim of this study was to uncover the effects of spatial frequency on both behavioural and neural responses to chromatic stimuli. We found reduced contrast sensitivity for high compared to low spatial frequency coloured gratings. Moreover, the decrease in sensitivity at high spatial frequencies was greater for gratings defined by S compared to L-M cone contrast. The BOLD responses we recorded from V1, V2 and V4 showed a significant interaction between spatial frequency of the target and chromatic condition, mirroring the behavioural results. This study suggests that neural responses to colour align well with behaviour in these areas.

The contrast sensitivity measures we obtained replicate a long-standing interaction between L-M and S-cone defined gratings and their spatial frequency (Mullen, 1985; Mullen and Kingdom, 2002; Poirson and Wandell, 1993, 1996, Welbourne, Morland and Wade, 2018). This shows that the RLM technique is capable of isolating chromatic mechanisms of human vision as others who devised the approach have shown in the past (Birch, Barbur & Harlow, 1992; Barbur, Birch and Harlow, 1993; Barbur, Harlow and Plant, 1994). We went further when we applied the RLM technique to measure brain responses. Measuring brain responses always comes with greater challenges because stimuli are presented at many times threshold and over a large area of visual field. For colour, this means that there is the potential for relatively large chromatic contrasts to generate small achromatic artefacts. Moreover, chromatic aberration can also play a role in generating luminance artefacts of coloured gratings, particularly at high spatial frequency

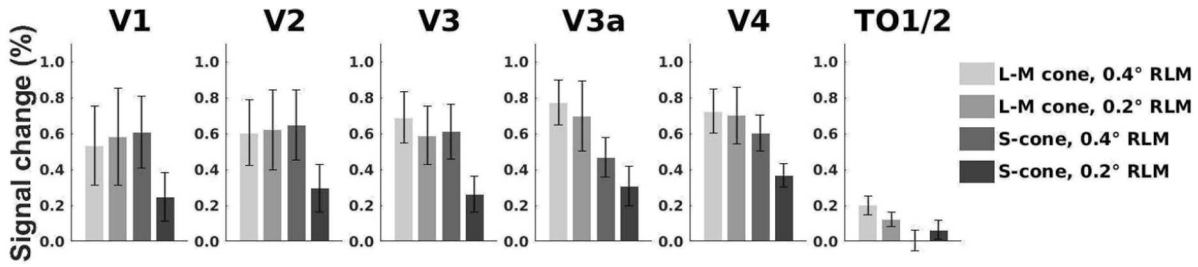

Fig. 7. A bar graph to show the mean percent signal change to the low spatial frequency target (1.25 cpd) on the low spatial frequency background (0.4 degrees squared checks) and the higher spatial frequency target (2.5 cpd) on the high spatial frequency background (0.2 degrees squared checks) for each colour direction (L-M and S-cone) for each visual area. Error bars are one SEM.

Table 3
Results of the ANOVA to investigate effects of visual areas (V1, V2, V3, V3a, hV4 and TO1/2), chromatic condition (L-M and S-cone) and spatial frequency when both targets were concordant with the RLM background (0.4 degrees squared checks with 1.25 cpd target and 0.2 degrees squared checks with 2.5 cpd target). Greenhouse-Geisser correction is applied when sphericity is violated.

Source	Mauchly's *p*	df1, df2	F	*p*	Effect Size
Area (A)	0.052	5, 25	6.10	**0.001**	0.55
Chromatic Condition (B)	.	1, 5	7.73	**0.039**	0.61
Spatial Frequency (C)	.	1, 5	4.19	0.096	0.46
A × B	**0.017**	1.86, 9.31	2.57	0.131	0.34
A × C	0.356	5, 25	5.22	**0.002**	0.51
B × C	.	1, 5	6.76	**0.048**	0.58
A × B × C	0.152	5, 25	7.06	**<0.001**	0.59

(Murasugi and Cavanagh, 1988, Bradley, Zhang and Thibos, 1992). Our result that gratings defined by a relatively high (15%) increment of achromatic contrast generated undetectable brain signals when presented on the randomly changing backgrounds suggests that any achromatic artefacts would not generate significant responses from cortex. This shows therefore that the RLM approach is well suited to studies of chromatic mechanisms, particularly for suprathreshold stimuli presented over a large area of the visual field. We note however that we did not account for each individual's macular pigment density, which could rotate the vector of the S-cone stimuli. However, this rotation is likely very small as variations in white points as a function of macular pigment density align closely with tritan confusion lines (Wright 1928–29, Ruddock, 1963).

Returning to the behavioural results, we replicated the lasting finding that there is lower sensitivity to S-cone stimuli than L-M stimuli in general and even more so at high spatial frequencies (Mullen, 1985; Mullen & Kingdom, 2002; Poirson & Wandell, 1993, 1996; Welbourne, Morland & Wade, 2018). Previous studies have suggested that S-cones have a lower response at all spatial frequencies due to a reduced quantum catch (Williams, Sekiguchi, & Brainard, 1993), but this does not explain the spatial frequency differences. Swanson (1996) showed that non-neural factors do not affect S-cone contrast sensitivity between 1 and 5 cpd, so these differences must be due to neural factors. The brain responses to coloured gratings depended both on their spatial frequency and colour as demonstrated by the interaction we have reported. This feature was most consistently observed in visual areas V1 and V2, but was also observed in hV4 in one but not another test. Previous work in our lab (Welbourne, Morland & Wade, 2018) has demonstrated decreased activity in V1 in high spatial frequency S-cone conditions when compared to L-M, but only at more peripheral eccentricities. Engel, Zhang and Wandell (1997) showed that responses in V1 aligned well with behaviour at 1 Hz temporal frequency, which is the same frequency we have used. There is also evidence that V1 is functionally linked with V2 and hV4 in a way that could explain the consistent interaction found in these areas in the current study. For example Nakamura and colleagues (1993) showed that in macaques, whilst V4 primarily receives input from V2, it also receives information directly from V1, bypassing V2. It also sends feedback projections to V1 and V2, as well as V3 (for review see Pasupathy, Popovkina & Kim, 2020). In humans, Wade and colleagues (2008, 2002) found significant responses to chromatic contrast across the ventral surface.

Although V3a exhibited a strong response to chromatic conditions, the interaction between chromatic condition and spatial frequency was not shown. V3a has been shown to have preference for achromatic stimuli and an enhanced response to flicker stimuli (Liu and Wandell, 2005). Therefore, the interaction between chromatic condition and spatial frequency may not be as salient in this area. In contrast to our work, previous work using an luminance modulated background found that chromatic responses were confined to the ventral surface (Wade et al., 2008), with no activation by chromatic stimuli of human dorsal areas like V3a. However, this study differed from ours in important ways that may explain the strong response we demonstrate in V3a. Firstly, the chromatic stimuli used in Wade and colleagues (2008) were defined as patches of colour and luminance, and had no spatial coherence unlike the gratings used in our study. Secondly, the chromatic target and achromatic background updated together at 1 Hz, so the temporal frequency of their achromatic and chromatic components were the same. V3a has been shown to be responsible for structure in motion processing (Koyama et al., 2005), so it is possible that our use of spatially structured grating and a temporally disparate stimulus has caused the colour to be perceived as a coherent separate stimulus that led to the response from V3a we have shown in this study.

TO1/2 showed very little response to any of our conditions, consistent with a motion selective and colour invariant area (Zeki et al., 1991). Previous work has shown fMRI responses in MT + to s-cone stimuli (Wandell et al., 1999), but this was 10 times lower than responses to achromatic stimuli, and the stimulus used in their experiment was low spatial frequency (0.5 cpd) and fast moving (8 degrees/second). In contrast, our stimuli were not moving, but phase shifting at a much lower rate (1 Hz) and our lowest spatial frequency grating was higher and thus not optimised for MT+. The research on MT+ is contentious about whether this area receives chromatic input at all (Zeki et al., 1991; Liu and Wandell, 2005) and our study suggests that it might not, or only when the chromatic information is at much lower spatial, but higher temporal, frequencies. Indeed, psychophysical studies have shown that when moving chromatic gratings are equated in luminance there is no visual perception of motion (Ramachandran and Gregory, 1978), lending support to the idea that MT+ does not receive chromatic input. Previous work relied on no, or suboptimal luminance masking to isolate chromatic stimuli (Wandell et al., 1999). Since MT+ is highly sensitive to even very low achromatic contrast, it is feasible that these previous results have been influenced by small luminance artefacts and chromatic aberration, which our study has accounted for using RLM.

hV4 has often been found to be a colour-specific area (Zeki et al., 1991; McKeefry & Zeki, 1997; Goddard et al., 2011) so it is interesting

that we did not find anything special about hV4 in this experiment. This research provides support for the suggestion that chromatic vision is more generally processed across the cortex, with some preferential processing in early areas V1 and V2 and ventral hV4. That we observed an interaction between spatial frequency and chromatic condition in V1, the lowest level of the cortical hierarchy, suggests that the neural mechanism could be set before the cortex, perhaps in the LGN or even colour opponent ganglion cells.

Psychophysical research has shown that colour perception is spatially low-pass at detection threshold (Mullen, 1985; Mullen and Kingdom, 2002; Poirson and Wandell, 1996; Welbourne, Morland and Wade, 2018) and for suprathreshold stimulus matching (Poirson and Wandell, 1993). In fMRI, V1 has also been shown to have spatially low-pass responses to colour stimuli when luminance is absent (Schluppeck and Engel, 2002). Both the behavioural and imaging studies are thought to be consistent with a low-pass single-opponent mechanism and our results add weight to this argument. It is also noted that there are double opponent cells in V1 that respond to both colour and luminance, but these exhibit band-pass characteristics, peaking at 2.56 cpd (Schluppeck and Engel, 2002). Such band pass mechanisms have recently been suggested to underpin the appearance of some structured chromatic stimuli (Shapley, Nunez and Gordon, 2019). However, our responses are far less likely to reflect these double opponent mechanisms because we record lower, not greater, responses to the 2.5 than the 1.25 cpd gratings.

We noted BOLD responses to S-cone stimuli at low spatial frequency were remarkably similar to those elicited by L-M stimuli. The cone contrasts of the stimuli eliciting these responses were however many more multiples of the psychophysically determined threshold for L-M than for S-cone stimuli. Mullen and colleagues (2007) also found surprisingly high S-cone responses in early visual areas relative to threshold, and found that cone contrast correlated better with BOLD response than a threshold based metric. Specifically, they found fMRI responses were just as robust for S-cone stimuli at 5 times threshold as L-M stimuli at 31 times threshold. Similarly, the current study has found similar BOLD responses to low spatial frequency S-cone stimuli at 6.17 times threshold as L-M stimuli at 20.95 times threshold. These results support the hypothesis that some contrast normalisation must be implemented for S-cone stimuli, leading to responses being amplified in V1 (Georgeson & Sullivan 1975, Heeger, 1992, Mullen et al., 2007, Carandini and Heeger, 2012).

5. Conclusions

This study has used RLM to provide support for previous work on colour contrast sensitivity, showing that colour vision is spatially low-pass, a finding which is reflected in fMRI BOLD responses in visual cortex. In V1, V2 and hV4, BOLD responses mirror behavioural data most consistently, showing that these areas are likely involved with colour perception. There is also some normalisation of S-cone signals across visual areas to make them more visible. The spatially low-pass nature of colour vision shown in this study provides support for work indicating that colour vision utilises single-opponent mechanisms. We have also found signals in the brain in early visual cortex that align well with behaviour, showing that chromatic responses are set early in the visual pathway, perhaps in the LGN.

CRediT authorship contribution statement

Rebecca Lowndes: Conceptualization, Methodology, Software, Investigation, Formal analysis, Data curation, Writing – original draft, Writing – review & editing. **Lauren Welbourne:** Formal analysis, Visualization. **Molly Williams:** Investigation. **Andre Gouws:** Software. **Alex Wade:** Supervision, Software, Writing – review & editing. **Antony Morland:** Conceptualization, Writing – review & editing, Methodology, Software, Investigation, Formal analysis, Supervision.

Declaration of Competing Interest

The authors declare that they have no known competing financial interests or personal relationships that could have appeared to influence the work reported in this paper.

Data availability

Data will be made available on request.

Acknowledgments

Supported by funding from BBSRC (BB/P007252).

References

Alvarez, I., De Haas, B. A., Clark, C. A., Rees, G., & Schwarzkopf, D. S. (2015). Comparing different stimulus configurations for population receptive field mapping in human fMRI. *Frontiers in Human Neuroscience, 9*(96), 1–16.

Amano, K., Wandell, B. A., & Dumoulin, S. O. (2009). Visual field maps, population receptive field sizes, and visual field coverage in the human MT+ complex. *Journal of Neurophysiology, 102*(5), 2704–2718.

Barbur, J. L., Birch, J., & Harlow, A. J. (1993). Colour vision testing using spatiotemporal luminance masking. In *Colour vision deficiencies XI* (pp. 417–426). Dordrecht: Springer.

Barbur, J. L., Harlow, J., & Plant, G. T. (1994). Insights into the different exploits of colour in the visual cortex. *Proceedings of the Royal Society of London. Series B: Biological Sciences*, *258*(1353), 327-334.

Benson, N. C., Butt, O. H., Brainard, D. H., & Aguirre, G. K. (2014). Correction of distortion in flattened representations of the cortical surface allows prediction of V1–V3 functional organization from anatomy. *PLoS Computational Biology, 10*(3), 1–9.

Benson, N. C., & Winawer, J. (2018). Bayesian analysis of retinotopic maps. *elife, 7*, 1–29.

Binda, P., Thomas, J. M., Boynton, G. M., & Fine, I. (2013). Minimizing biases in estimating the reorganization of human visual areas with BOLD retinotopic mapping. *Journal of Vision, 13*(7), 1–16.

Birch, J., Barbur, J. L., & Harlow, A. J. (1992). New method based on random luminance masking for measuring isochromatic zones using high resolution colour displays. *Ophthalmic and Physiological Optics, 12*(2), 133–136.

Bowmaker, J. K., & Dartnall, H. (1980). Visual pigments of rods and cones in a human retina. *The Journal of Physiology, 298*(1), 501–511.

Bradley, A., Zhang, X., & Thibos, L. (1992). Failures of isoluminance caused by ocular chromatic aberrations. *Applied Optics, 31*(19), 3657–3667.

Brown, P. K., & Wald, G. (1964). Visual pigments in single rods and cones of the human retina. *Science, 144*(3614), 45–52.

Carandini, M., & Heeger, D. J. (2012). Normalization as a canonical neural computation. *Nature Reviews Neuroscience, 13*(1), 51–62.

Castaldi, E., Frijia, F., Montanaro, D., Tosetti, M., & Morrone, M. C. (2013). BOLD human responses to chromatic spatial features. *European Journal of Neuroscience, 38*(2), 2290–2299.

Chen, S. F., Chang, Y., & Wu, J. C. (2001). The spatial distribution of macular pigment in humans. *Current Eye Research, 23*(6), 422–434.

Conway, B. R. (2009). Color vision, cones, and color-coding in the cortex. *The Neuroscientist, 15*(3), 274–290.

Dale, A. M., Fischl, B., & Sereno, M. I. (1999). Cortical surface-based analysis: I. Segmentation and surface reconstruction. *Neuroimage, 9*(2), 179–194.

Davies, N. P., & Morland, A. B. (2004). Macular pigments: Their characteristics and putative role. *Progress in Retinal and Eye Research, 23*(5), 533–559.

Derrington, A. M., Krauskopf, J., & Lennie, P. (1984). Chromatic mechanisms in lateral geniculate nucleus of macaque. *The Journal of physiology, 357*(1), 241–265.

DeYoe, E. A., Bandettini, P., Neitz, J., Miller, D., & Winans, P. (1994). Functional magnetic resonance imaging (FMRI) of the human brain. *Journal of Neuroscience Methods, 54*(2), 171–187.

Dougherty, R. F., Koch, V. M., Brewer, A. A., Fischer, B., Modersitzki, J., & Wandell, B. A. (2003). Visual field representations and locations of visual areas V1/2/3 in human visual cortex. *Journal of Vision, 3*(10), 586–598.

D'Souza, D. V., Auer, T., Strasburger, H., Frahm, J., & Lee, B. B. (2011). Temporal frequency and chromatic processing in humans: An fMRI study of the cortical visual areas. *Journal of Vision, 11*(8), 1–17.

Dumoulin, S. O., & Wandell, B. A. (2008). Population receptive field estimates in human visual cortex. *NeuroImage, 39*(2), 647–660.

Engel, S. A., Glover, G. H., & Wandell, B. A. (1997). Retinotopic organization in human visual cortex and the spatial precision of functional MRI. *Cerebral cortex (New York, NY: 1991)*, *7*(2), 181-192.

Engel, S., Zhang, X., & Wandell, B. (1997). Colour tuning in human visual cortex measured with functional magnetic resonance imaging. *Nature, 388*(6637), 68–71.

Georgeson, M. A., & Sullivan, G. D. (1975). Contrast constancy: Deblurring in human vision by spatial frequency channels. *The Journal of Physiology, 252*(3), 627–656.

Glasser, M. F., Sotiropoulos, S. N., Wilson, J. A., Coalson, T. S., Fischl, B., Andersson, J. L., ... & Wu-Minn HCP Consortium. (2013). The minimal preprocessing pipelines for the Human Connectome Project. *Neuroimage*, *80*, 105-124.

Goddard, E., Mannion, D. J., McDonald, J. S., Solomon, S. G., & Clifford, C. W. (2011). Color responsiveness argues against a dorsal component of human V4. *Journal of Vision, 11*(4), 1–21.
Goodchild, A. K., Ghosh, K. K., & Martin, P. R. (1996). Comparison of photoreceptor spatial density and ganglion cell morphology in the retina of human, macaque monkey, cat, and the marmoset Callithrix jacchus. *Journal of Comparative Neurology, 366*(1), 55–75.
Hammond, B. R., Wooten, B. R., & Snodderly, D. M. (1997). Individual variations in the spatial profile of human macular pigment. *JOSA A, 14*(6), 1187–1196.
Heeger, D. J. (1992). Normalization of cell responses in cat striate cortex. *Vis. Neurosci., 9*, 181–197.
Jenkinson, M., & Smith, S. (2001). A global optimisation method for robust affine registration of brain images. *Medical Image Analysis, 5*(2), 143–156.
Jenkinson, M., Bannister, P., Brady, M., & Smith, S. (2002). Improved optimization for the robust and accurate linear registration and motion correction of brain images. *Neuroimage, 17*(2), 825–841.
Kim, Y. J., Reynaud, A., Hess, R. F., & Mullen, K. T. (2017). A normative data set for the clinical assessment of achromatic and chromatic contrast sensitivity using a qCSF approach. *Investigative Ophthalmology & Visual Science, 58*(9), 3628–3636.
Klaver, P., Lichtensteiger, J., Bucher, K., Dietrich, T., Loenneker, T., & Martin, E. (2008). Dorsal stream development in motion and structure-from-motion perception. *Neuroimage, 39*(4), 1815–1823.
Koyama, S., Sasaki, Y., Andersen, G. J., Tootell, R. B., Matsuura, M., & Watanabe, T. (2005). Separate processing of different global-motion structures in visual cortex is revealed by FMRI. *Current Biology, 15*(22), 2027–2032.
Liu, J., & Wandell, B. A. (2005). Specializations for chromatic and temporal signals in human visual cortex. *The Journal of Neuroscience, 25*, 3459–3468.
MacLeod, D. I., & Boynton, R. M. (1979). Chromaticity diagram showing cone excitation by stimuli of equal luminance. *JOSA, 69*(8), 1183–1186.
McKeefry, D. J., & Zeki, S. (1997). The position and topography of the human colour centre as revealed by functional magnetic resonance imaging. *Brain: A Journal of Neurology, 120*(12), 2229–2242.
Mikellidou, K., Frijia, F., Montanaro, D., Greco, V., Burr, D. C., & Morrone, M. C. (2018). Cortical BOLD responses to moderate-and high-speed motion in the human visual cortex. *Scientific Reports, 8*(1), 1–12.
Mullen, K. T. (1985). The contrast sensitivity of human colour vision to red-green and blue-yellow chromatic gratings. *The Journal of Physiology, 359*(1), 381–400.
Mullen, K. T. (2019). The response to colour in the human visual cortex: The fMRI approach. *Current Opinion in Behavioral Sciences, 30*, 141–148.
Mullen, K. T., Dumoulin, S. O., McMahon, K. L., De Zubicaray, G. I., & Hess, R. F. (2007). Selectivity of human retinotopic visual cortex to S-cone-opponent, L/M-cone-opponent and achromatic stimulation. *European Journal of Neuroscience, 25*(2), 491–502.
Mullen, K. T., & Kingdom, F. A. A. (2002). Differential distributions of red–green and blue–yellow cone opponency across the visual field. *Visual Neuroscience, 19*(1), 109–118.
Mullen, K. T., Thompson, B., & Hess, R. F. (2010). Responses of the human visual cortex and LGN to achromatic and chromatic temporal modulations: An fMRI study. *Journal Vision, 10*(13), 1–19.
Mullen, K. T., Chang, D. H., & Hess, R. F. (2015). The selectivity of responses to red-green colour and achromatic contrast in the human visual cortex: An fMRI adaptation study. *European Journal of Neuroscience, 42*(11), 2923–2933.
Murasugi, C. M., & Cavanagh, P. (1988). Anisotropy in the chromatic channel: A horizontal-vertical. *Spatial Vision, 3*(4), 281–291.
Neitz, A., Jiang, X., Kuchenbecker, J. A., Domdei, N., Harmening, W., Yan, H., … Sabesan, R. (2020). Effect of cone spectral topography on chromatic detection sensitivity. *JOSA A, 37*(4), 1–24.
Nestares, O., & Heeger, D. J. (2000). Robust multiresolution alignment of MRI brain volumes. *Magnetic Resonance in Medicine: An Official Journal of the International Society for Magnetic Resonance in Medicine, 43*(5), 705–715.
Pasupathy, A., Popovkina, D. V., & Kim, T. (2020). Visual functions of primate area V4. *Annual Review of Vision Science, 6*, 363–385.
Pefferkorn, S., Chiron, A., & Viénot, F. (1997). *Effect of longitudinal chromatic aberration on photometric matches using a heterochromatic square-wave grating. In Colour Vision Deficiencies XIII* (pp. 403–407). Dordrecht: Springer.
Poirson, A. B., & Wandell, B. A. (1993). Appearance of colored patterns: Pattern–color separability. *JOSA A, 10*(12), 2458–2470.
Poirson, A. B., & Wandell, B. A. (1996). Pattern—color separable pathways predict sensitivity to simple colored patterns. *Vision Research, 36*(4), 515–526.
Railo, H., Salminen-Vaparanta, N., Henriksson, L., Revonsuo, A., & Koivisto, M. (2012). Unconscious and conscious processing of color rely on activity in early visual cortex: A TMS study. *Journal of Cognitive Neuroscience, 24*(4), 819–829.
Ramachandran, V. S., & Gregory, R. L. (1978). Does colour provide an input to human motion perception? *Nature, 275*(5675), 55–56.
Regan, D., & He, P. (1996). Magnetic and electrical brain responses to chromatic contrast in human. *Vision Research, 36*(1), 1–18.
Reuter, M., Schmansky, N. J., Rosas, H. D., & Fischl, B. (2012). Within-subject template estimation for unbiased longitudinal image analysis. *Neuroimage, 61*(4), 1402–1418.
Ruddock, K. H. (1963). Evidence for macular pigmentation from colour matching data. *Vision Research, 3*(9–10), 417–429.
Rynders, M. C., Navarro, R., & Losada, M. A. (1998). Objective measurement of the off-axis longitudinal chromatic aberration in the human eye. *Vision Research, 38*(4), 513–522.
Schluppeck, D., & Engel, S. A. (2002). Color opponent neurons in V1: A review and model reconciling results from imaging and single-unit recording. *Journal of Vision, 2*(6), 480–492.
Sereno, M. I., Dale, A. M., Reppas, J. B., Kwong, K. K., Belliveau, J. W., Brady, T. J., … Tootell, R. B. H. (1995). Borders of multiple visual areas in humans revealed by functional magnetic resonance imaging. *Science, 268*(5212), 889–893.
Shapley, R., Nunez, V., & Gordon, J. (2019). Cortical double-opponent cells and human color perception. *Current Opinion in Behavioral Sciences, 30*, 1–7.
Smith, S. M. (2002). Fast robust automated brain extraction. *Human Brain Mapping, 17*(3), 143–155.
Smith, S. M., Jenkinson, M., Woolrich, M. W., Beckmann, C. F., Behrens, T. E., Johansen-Berg, H., … Matthews, P. M. (2004). Advances in functional and structural MR image analysis and implementation as FSL. *Neuroimage, 23*, S208–S219.
Snodderly, D. M., Auran, J. D., & Delori, F. C. (1984). The macular pigment. II. Spatial distribution in primate retinas. *Investigative Ophthalmology & Visual Science, 25*(6), 674–685.
Srinivasan, V. J., Monson, B. K., Wojtkowski, M., Bilonick, R. A., Gorczynska, I., Chen, R., … Fujimoto, J. G. (2008). Characterization of outer retinal morphology with high-speed, ultrahigh-resolution optical coherence tomography. *Investigative Ophthalmology & Visual Science, 49*(4), 1571–1579.
Stiles, W. S. (1946). Separation of the 'blue'and 'green'mechanisms of foveal vision by measurements of increment thresholds. *Proceedings of the Royal Society of London. Series B-Biological Sciences, 133*(873), 418-434.
Stockman, A., & Sharpe, L. T. (2000). Tritanopic color matches and the middle-and long-wavelength-sensitive cone spectral sensitivities. *Vision Research, 40*(13), 1739–1750.
Strasburger, H., Bach, M., & Heinrich, S. P. (2018). Blur unblurred—a mini tutorial. *i-Perception, 9*(2), 1–15.
Swanson, W. H. (1996). S-cone spatial contrast sensitivity can be independent of pre-receptoral factors. *Vision Research, 36*(21), 3549–3555.
Tootell, R. B., Mendola, J. D., Hadjikhani, N. K., Ledden, P. J., Liu, A. K., Reppas, J. B., … Dale, A. M. (1997). Functional analysis of V3A and related areas in human visual cortex. *Journal of Neuroscience, 17*(18), 7060–7078.
Von Helmholtz, H. (1867). *Treatise on Physiological Optics* (vol. iii). translated by J. P. C. Southall, Opt.Soc. Am., 1924–5.
Wade, A. R., Brewer, A. A., Rieger, J. W., & Wandell, B. A. (2002). Functional measurements of human ventral occipital cortex: Retinotopy and colour. *Philosophical Transactions of the Royal Society of London. Series B: Biological Sciences, 357*(1424), 963–973.
Wade, A., Augath, M., Logothetis, N., & Wandell, B. (2008). fMRI measurements of color in macaque and human. *Journal of vision, 8*(10), 1–19.
Wandell, B. A., Poirson, A. B., Newsome, W. T., Baseler, H. A., Boynton, G. M., Huk, A., … Sharpe, L. T. (1999). Color signals in human motion-selective cortex. *Neuron, 24*(4), 901–909.
Wiesel, T. N., & Hubel, D. H. (1966). Spatial and chromatic interactions in the lateral geniculate body of the rhesus monkey. *Journal of Neurophysiology, 29*(6), 1115–1156.
Welbourne, L. E., Morland, A. B., & Wade, A. R. (2018). Population receptive field (pRF) measurements of chromatic responses in human visual cortex using fMRI. *NeuroImage, 167*, 84–94.
Williams, D., Sekiguchi, N., & Brainard, D. (1993). Color, contrast sensitivity, and the cone mosaic. *Proceedings of the National Academy of Sciences, 90*(21), 9770–9777.
Woolrich, M. W., Ripley, B. D., Brady, M., & Smith, S. M. (2001). Temporal autocorrelation in univariate linear modeling of FMRI data. *Neuroimage, 14*(6), 1370–1386.
Wright, W. D. (1928-29) A re-determination of the trichromatic coefficients of the spectral colours. *Transactions of the Optical Society 30*(4), 141-164.
Wuerger, S., Ashraf, M., Kim, M., Martinovic, J., Pérez-Ortiz, M., & Mantiuk, R. K. (2020). Spatio-chromatic contrast sensitivity under mesopic and photopic light levels. *Journal of Vision, 20*(4), 1–26.
Young, T. (1802). II. The Bakerian Lecture. On the theory of light and colours. *Philosophical transactions of the Royal Society of London, 92*, 12–48.
Zeki, S., Watson, J. D., Lueck, C. J., Friston, K. J., Kennard, C., & Frackowiak, R. S. (1991). A direct demonstration of functional specialization in human visual cortex. *Journal of Neuroscience, 11*(3), 641–649.